

# Influence and Suppression of Harmful Effects Due to By-Product in CVD Reactor for 4H-SiC Epitaxy

Yoshiaki Daigo<sup>1</sup>, Toru Watanabe<sup>1</sup>, Akio Ishiguro, Shigeaki Ishii, and Yoshikazu Moriyama

**Abstract**—Suppression of harmful effect due to by-product on homo-epitaxial growth of 4H-SiC films using a high speed wafer rotation vertical CVD method was demonstrated. Influence of by-product, such as 3C-SiC deposit on a hot-wall and Si deposit on gas nozzles, formed during the epitaxial growth was investigated in two comparative studies. The analysis of triangular defects with 3C-SiC down-falls on the films revealed that the most of the down-falls which were peeled from the hot-wall adhered to the wafers before the epitaxial growth. By increasing the wafer rotation speed to 300 rpm just after wafer loading into the reactor, the down-falls dropped towards the wafer surface were effectively eliminated, and the maintenance period of the reactor could be increased more than 4 times compared to the case of maintaining the wafer rotation speed of 50 rpm until just before epitaxial growth step. Additionally, the relationship between Si deposit formed on the gas nozzles in the gas inlet and fluctuation of thickness and doping concentration of the films suggested that Si deposit formed on the gas nozzles acts as a trap site of Si source gas. By suppression of the Si deposit using optimizing gas flow condition, no significant fluctuation of thickness and doping concentration of the films were observed and the maintenance period of the gas nozzles could be increased more than 3 times compared to the epitaxial growth using the nozzles on which Si deposit was formed.

**Index Terms**—4H-SiC, epitaxial growth, by-product, down-fall, repeatability, growth rate, doping concentration.

## I. INTRODUCTION

4H-SiC is expected as a material for achieving power devices operated under high current density and high voltage, because of its excellent physical properties such as wide band gap, high thermal conductivity and high breakdown electric field. Schottky barrier diodes [1]–[3] and metal-oxide-semiconductor field-effect transistors [2]–[5] based on the 4H-SiC, which have high breakdown voltage around 0.6–1.7 kV, have already been put to practical use. In order to realize the power devices operated under higher current density and higher voltage, bipolar devices in which lower on-resistance can be achieved by conductivity modulation are also studied all over the world [6]–[8].

Manuscript received February 15, 2021; revised April 12, 2021; accepted April 26, 2021. Date of publication May 5, 2021; date of current version August 4, 2021. (Corresponding author: Yoshiaki Daigo.)

The authors are with TFW Equipment Engineering Department, NuFlare Technology, Inc., Yokohama 235-8522, Japan (e-mail: daigo.yoshiaki@nuf flare.co.jp; watanabe.toru@nuf flare.co.jp; ishiguro.akio@nuf flare.co.jp; ishii.shigeaki@nuf flare.co.jp; moriyama.yoshikazu@nuf flare.co.jp).

Color versions of one or more figures in this article are available at <https://doi.org/10.1109/TSM.2021.3077627>.

Digital Object Identifier 10.1109/TSM.2021.3077627

In the fabrication of the power devices based on the 4H-SiC, a CVD method used for homo-epitaxial growth of drift layer and buffer layer on the 4H-SiC substrate is one of the key technologies. Reducing the defects in epitaxial films is still the main issue for device fabrication, because the defects originated from the substrates and in-grown defects have harmful effects on the reliability of SiC devices [9]–[12]. Since the wafer is still expensive, repeatability and uniformity of thickness and doping concentration of the epitaxial films on a large diameter wafers are also required for the cost reduction of device fabrication.

Moreover, since a thick drift layer of at least 10  $\mu\text{m}$  or more is required for most of the SiC power devices, a large amount of by-product due to iteration of epitaxial growth are formed in CVD reactor, having harmful effect on epitaxial growth [13], [14]. In order to reduce the harmful effect on the epitaxial growth due to by-product in the reactor, short maintenance period is required for mass production of 4H-SiC epitaxial films, resulting obstacles to high productivity. Unfortunately, the generation mechanism and its influence of by-product have not been fully investigated, and the technique to reduce the harmful effect due to by-product have not been sufficiently proposed.

Previously, the authors reported that the influence of by-product in CVD reactor on the epitaxial growth of the 4H-SiC films were investigated in two comparative studies. One of them is the comparison of two different process sequence for the influence of down-fall density on the films due to 3C-SiC deposit formed on hot-wall [15], [16]. Another of them is the comparison of two different condition for the influence of thickness and doping concentration of the films due to Si deposit formed on gas nozzles in gas inlet [15]. In this paper, detailed mechanism of the harmful effects due to by-product in CVD reactor and their detailed suppression models are investigated.

## II. EXPERIMENTAL DETAILS

### A. Epitaxial Growth of 4H-SiC Films

In this study, n-type 4H-SiC epitaxial films were grown on 4H-SiC wafers (150 mm diameter, Si face, 4° off) using high speed wafer rotation vertical CVD tool shown in Fig. 1. The wafers are placed on a susceptor which is set on a rotation holder, and are heated by the upper resistive heaters and lower resistive heaters through the hot-wall and the susceptor, respectively. The temperature at center and edge of the wafer can be monitored by two pyrometers, and can be controlled

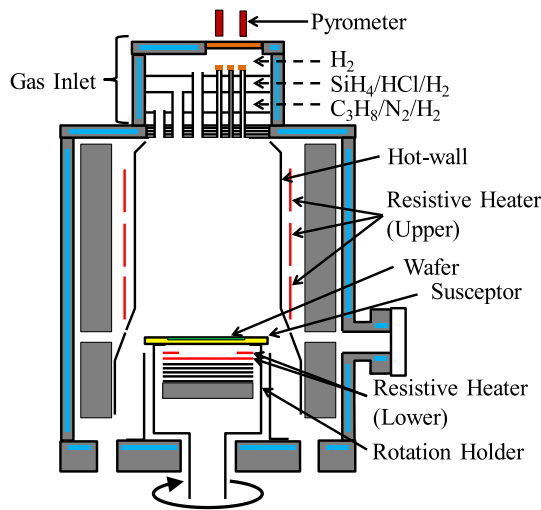


Fig. 1. Schematic illustration of CVD reactor used in this study.

independently by using temperature feedback system. The gas inlet is placed on the top of the reactor, and process gases are introduced into the reaction space through the gas nozzles in the gas inlet. Typical rotation speed and typical growth temperature during the epitaxial growth are 600 rpm and 1625 °C, respectively. SiH<sub>4</sub>, C<sub>3</sub>H<sub>8</sub>, HCl, N<sub>2</sub> and H<sub>2</sub> gases are used as process gases, and SiH<sub>4</sub> and C<sub>3</sub>H<sub>8</sub> gases are introduced separately into the reactor.

Figure 2 shows process sequence image of epitaxial growth of 4H-SiC films. In this figure, process sequence of wafer temperature (a), heater power (b) and wafer rotation speed (c) from the wafer loading step to epitaxial growth step are shown. First, rotation speed is increased just after the wafer loading into the reactor. Next, wafer temperature is increased by increasing the heater power. Then, H<sub>2</sub> etching of the wafer surface are performed at the same temperature with epitaxial growth. Finally, just after H<sub>2</sub> etching, epitaxial growth is performed under the rotation speed of 600 rpm.

In the first experiment, long term influence of rotational speed during the heat up step on down-fall density was investigated. Since the short term influence of rotational speed during the heat up step on down-fall density has been reported, the rotational speed during the heat-up step was set at 50 and 300 rpm based on the previous report [16].

### B. Characterization of 4H-SiC Films

The film thickness and the doping concentration of the films were evaluated by Fourier Transform Infrared spectroscopy (FT-IR) and mercury probe capacitance-voltage (Hg-CV) measurement. FT-IR measurement was performed under approximately  $\phi$  2.0 mm spot size on the wafer and the film thickness was calculated in the wave number range of 1700-3500cm<sup>-1</sup>. Hg-CV measurement was performed under approximately  $\phi$  1.6 mm spot size on the wafer and the doping concentration was measured at a frequency of 500 Hz. Both measurements were performed along  $\langle 11-20 \rangle$  and  $\langle -1100 \rangle$  directions on the 4H-SiC epitaxial wafers under the edge exclusion of 5.0 mm.

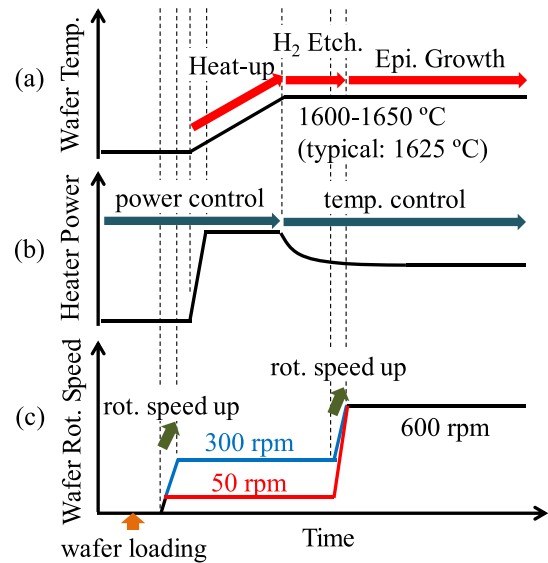


Fig. 2. Process sequence of epitaxial growth of 4H-SiC films. In this figure, process sequence of wafer temperature (a), heater power (b) and wafer rotation speed (c) from the wafer loading to epitaxial growth was described. Some parts of this figure were referred from literature [16].

Defects on the films were evaluated by using automatic inspection equipment based on confocal differential interference contrast (CDIC) microscope. After the inspection for epitaxial wafers, photo images on the whole wafers were reviewed and the misclassification of the defects consist of down-falls were corrected.

## III. RESULTS AND DISCUSSION

### A. Influence of 3C-SiC Deposit Formed on a Hot-WALL

In the reactor to grow 4H-SiC films, it is well known that a large amount of by-product consists of 3C-SiC crystals are formed on the wall in the reactor, and down-fall defects and/or triangular defects with down-fall due to peeling of the 3C-SiC deposit are formed on the film [10]. These defects are the most serious device killer defects, and the reduction of these defects is important. Therefore, influence of 3C-SiC deposit formed on hot-wall in the reactor was investigated.

Figure 3 shows photo image of triangular defect with down-fall. It was found that the triangular defect originated from down-fall are formed towards downstream side of step flow growth direction from the down-fall. Additionally, the triangular defect shown in Fig. 3 (a) seems to consist of three triangular structures. If these structures correspond to pure triangle shape, the length of these structures are 156, 172, and 173  $\mu$ m, as shown by the dashed lines in Fig. 3 (b). Basically, the triangular defect with down-fall is formed above the stacking fault originated from the down-fall, and the stacking fault is extended to downstream side along the basal plane of the substrate [17]. Additionally, the homo-epitaxial growth of 4H-SiC is generally performed using off-axis substrate and the length of the triangular defect is determined from the relationship between the thickness and off angle of the substrate.

Figure 4 shows schematic illustrations of formation mechanism of triangular defect originated from down-fall. As shown

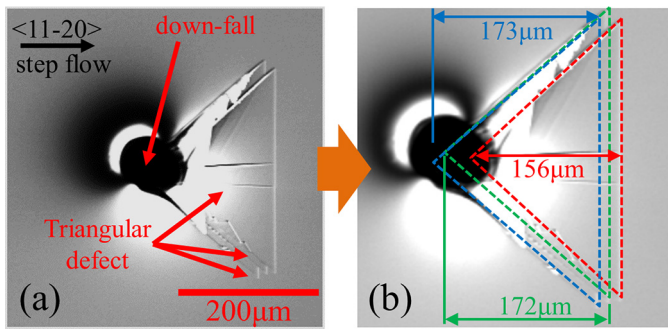


Fig. 3. Photo image of triangular defect with down-fall. The appearance of fitting to three different triangular structures is shown in (b).

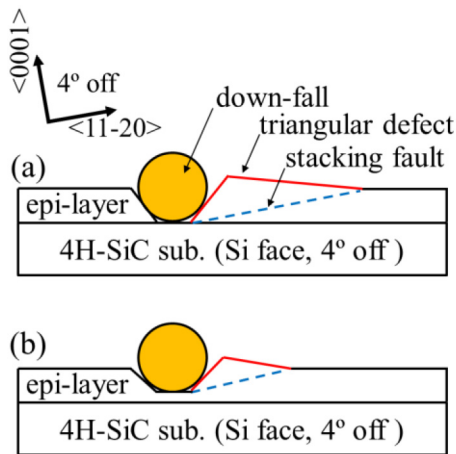


Fig. 4. Schematic illustrations of formation mechanism of triangular defect with down-fall. Triangular defect with down-fall formed at initial stage of epitaxial growth (a) and at middle of epitaxial growth (b).

in Fig. 4 (a) and (b), the length of the stacking fault and triangular defect with down-fall depends on the film thickness above from the defect origin such as down-fall. Since the 4H-SiC film shown in Fig. 3 was grown on  $4^\circ$  off wafers with film thickness of  $10.5 \mu\text{m}$ , the length of a triangular structure of  $156 \mu\text{m}$  corresponds to that of the defect generated from the interface between epitaxial layer and substrate. Since the origin of the triangular structures are covered with down-fall, two larger values, such as  $171$  and  $172 \mu\text{m}$ , which are larger than the thickness from the substrate interface to the surface of the film, are believed to be due to fitting errors in the dashed line shown in Fig. 3 (b).

Figure 5 shows typical down-fall map for the SiC film measured by automatic inspection equipment based on CDIC microscope. On this map, defect density of down-falls was  $0.31 \text{ cm}^{-2}$ , and all 50 down-fall defects were accompanied by triangular defects and no pure downfall defects were observed.

Figure 6 shows the histogram of length of triangular defect with down-fall on the wafer shown in Fig. 5. When the triangular defect is accompanied by a multiple triangular structures as described in Fig. 3, the length was measured for the most downstream triangular structure in the step flow growth direction. The length of triangular defect was distributed in a range of  $135$  to  $170 \mu\text{m}$ , and average was  $149 \mu\text{m}$ . Since the film thickness of the film shown in Fig. 5 was  $11.2 \mu\text{m}$ , the

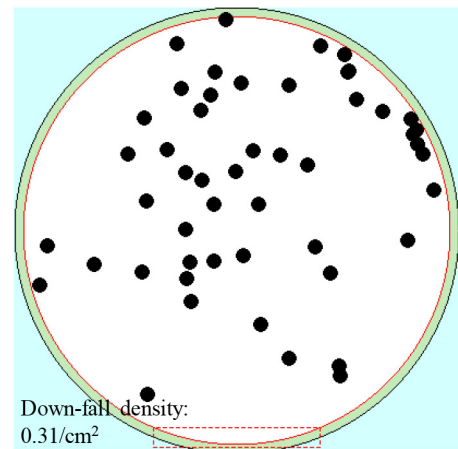


Fig. 5. Typical down-fall map measured by automatic inspection equipment based on CDIC microscope. In this map, 50 triangular defects with down-falls were observed, and pure down-fall defect including triangular defect were not observed.

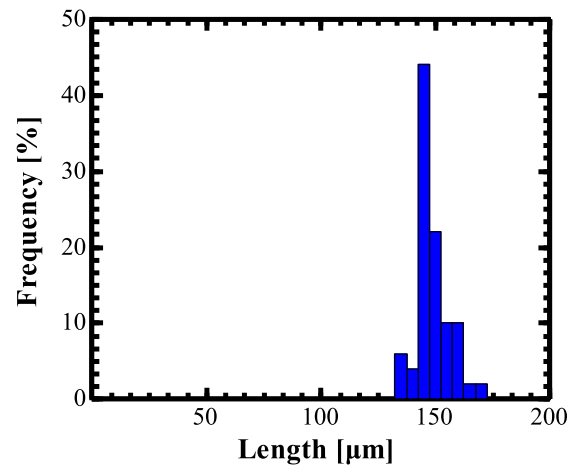


Fig. 6. Histogram of length of triangular defect with down-fall on the wafer shown in Fig. 5.

length measured likely corresponds to the thickness from the substrate interface to the surface of the film.

As the result of confirmation to many other wafers used in this study, it was found that there were few down-falls without triangular defects, and in most case, the triangular defect with down-fall was generated from the interface between epitaxial layer and substrate. These findings suggest that most of down-falls were dropped from the hot-wall before the epitaxial growth, such as wafer loading step, heat-up step and/or  $\text{H}_2$  etching step, shown in Fig. 2.

High speed wafer rotation vertical CVD method seems to have advantage for down-fall reduction compared with other growth method. Figure 7 shows schematic illustration of two possible models of down-fall reduction on the wafer. The inserted photo image is 3C-SiC deposit formed on the hot wall. The 3C-SiC deposit shown in the inserted photo image is formed on hot-wall, some of which are dropped towards the wafer surface as 3C-SiC particles. However, since the high-speed rotation creates a fast gas flow on the wafer surface from the inside to the outside of the wafer, it is possible that 3C-SiC particles are eliminated to the out of the wafer. In

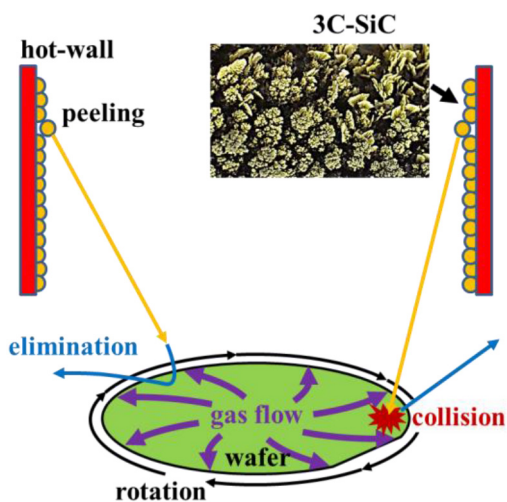


Fig. 7. Two possible models of down-fall reduction on the wafer. The inserted photo image is 3C-SiC deposit formed on the hot wall.

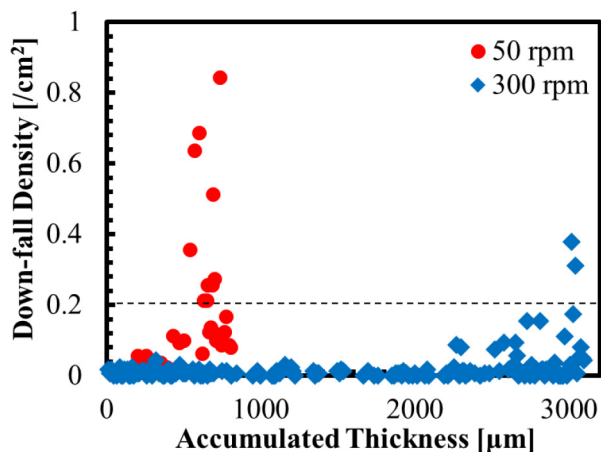


Fig. 8. Relationship between accumulated thickness in the reactor and the down-fall density on the films grown by the process sequence shown in Fig. 7, which was obtained by a long-term experiment.

addition, collision with high-speed rotating wafer might cause the elimination of 3C-SiC particles to the out of the wafer. By using this technique, it is possible to maintain a low down-fall density even if the accumulated thickness of the reactor increases.

Figure 8 shows relationship between accumulated thickness in the reactor and the down-fall density on the films grown by the process sequence shown in Fig. 2, which was obtained by a long term experiment. Needless to say, the down-fall density in Fig. 8 contains the density of triangular defects with down-fall, rather, it is dominant. In case of the process sequence in which the rotation speed at heat-up step is 50 rpm, the down-fall density was increased considerably at accumulated thickness more than 500  $\mu\text{m}$ . In case of the process sequence in which the rotation speed at heat-up step is 300 rpm, the down-fall density less than  $0.2\text{ cm}^{-2}$  was maintained up to the accumulated thickness of 3000  $\mu\text{m}$ . The maintenance period of the reactor under the rotation speed at heat-up step could be increased more than 4 times compared with wafer rotation speed of 50 rpm during the heat-up step. Therefore, the high

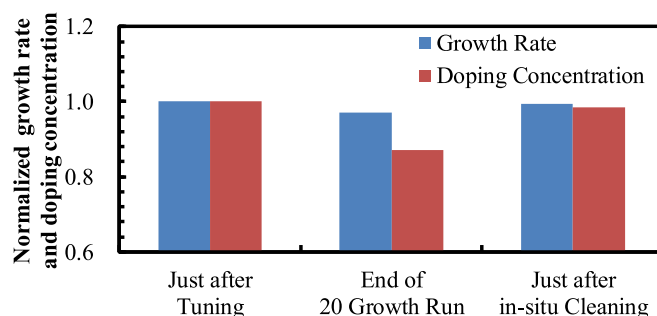


Fig. 9. Normalized growth rate and doping concentration of the tree SiC films grown by same recipe. The SiC films were grown just after final process tuning (a), at the end of 20 consecutive growth run (b) and just after in-situ reactor cleaning (c).

speed wafer rotation CVD can be proposed as a very useful technology for improving productivity of 4H-SiC films.

These results indicate the 3C-SiC deposit on the hot-wall was peeled off and a large amount of 3C-SiC particles were generated in the reactor with accumulated thickness more than 500  $\mu\text{m}$ . Additionally, it is also suggested 3C-SiC particles were effectively eliminated to the out of the wafer by using the process sequence in which the rotation speed at heat-up step is 300 rpm, even though the a large amount of 3C-SiC particles were generated in the reactor with accumulated thickness more than 500  $\mu\text{m}$ . Since the hot-wall consists of carbon material, fluctuation of the strain induced at interface between hot-wall and 3C-SiC deposit is likely to occur in the heat-up step. Therefore, the advantage on the rotation speed of 300 rpm at heat-up step is thought to be caused by larger elimination force, as shown in Fig. 7, in the timing of 3C-SiC particle generation.

#### B. Influence of Si Deposit Formed on the Gas Nozzles

In the vertical CVD reactor to grow 4H-SiC films, it is known that parasitic deposition is likely to be formed at around gas inlet which is heated by radiation from the high temperature wafer and hot-wall. It has been reported that Si droplets and SiC particles are attached to the wafer due to by-product formed in the gas inlet [14]. In this paper, halogenated Si precursors instead of  $\text{SiH}_4$  gas was proposed to reduce the by-product formed in the gas inlet. However,  $\text{SiH}_4$  gas is most commonly used for 4H-SiC epitaxial growth, it is important to evaluate and to reduce the harmful effect of by-product at around gas inlet on 4H-SiC epitaxial growth using conventional gases. In this study, therefore, influence of by-product formed at around gas inlet using  $\text{SiH}_4$  gas as Si precursors was investigated.

Figure 9 shows normalized growth rate and normalized doping concentration for three SiC films which were grown by same recipe. First of them was grown just after final process tuning which were performed before the consecutive growth run. Second of them was grown at the end of 20 consecutive growth run which were performed just after final process tuning. Third of them was grown at just after in-situ reactor cleaning which was performed through further 6 different growth run after 20 consecutive growth run. As shown in Fig. 9, it was found that thickness and doping concentration of

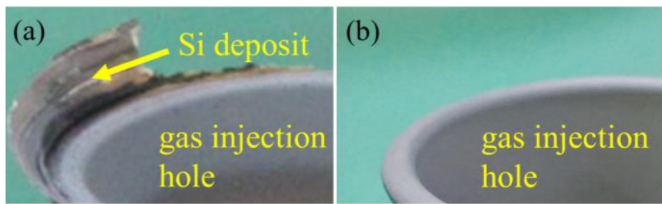


Fig. 10. Photo images of tip of gas nozzles used under un-optimized (previous) condition (a) and optimized condition (b).

the film grown just after process tuning cannot be maintained until end of 20 consecutive growth run. However, those were recovered just after in-situ reactor cleaning.

To investigate the reason of these fluctuation, a long-term iteration of epitaxial growth without in-situ cleaning was performed before the confirming the inside of the reactor. Figure 10 shows photo image of tip of gas nozzles in gas inlet, which are placed in top of the reactor, as shown in Fig. 1. Figure 10 (a) is gas nozzle used for a long-term iteration of epitaxial growth without in-situ cleaning, and it was found that the Si deposit is formed on the gas nozzles. If decrease of growth rate and doping concentration after the 20 consecutive growth run shown in Fig. 9 correlates Si deposit on the nozzles, the recovery of them just after in-situ cleaning thought to be due to the effect of reducing the Si deposit on the gas nozzles. Therefore, growth condition to suppress the Si deposit on the gas nozzles were investigated. Figure 10 (b) shows the gas nozzle used under the optimized condition, such as gas flow and temperature at around gas inlet. The nozzle was used for a long-term iteration of epitaxial growth without in-situ cleaning. By optimizing those conditions, it was revealed that the Si deposit is completely suppressed.

Figure 11 shows repeatability of growth rate of the SiC films grown under optimized and un-optimized (previous) conditions. Same recipes were used in each growth runs, and additional treatments, such as reactor cleaning, were not performed within each growth runs. Figure 12 shows repeatability of doping concentration of the SiC films shown in Fig. 11. Since the target value of doping concentration was different between two growth runs, doping concentration value was divided by  $N_2$  flow rate in this figure. Under the optimized condition, gas flow and temperature at around gas inlet had been tuned.

As shown in Figs. 11 and 12, the growth rate and doping concentration of the films grown under the un-optimized condition were decreased at accumulated thickness more than 150  $\mu\text{m}$ . In addition, after the growth runs under un-optimized condition, it was confirmed that Si deposit similar to that shown in Fig. 10 (a) are formed on the gas nozzles. On the other hand, it was found that extremely low fluctuation of the growth rate and the doping concentration for the films grown under the optimized condition is maintained up to the accumulated thickness of about 500  $\mu\text{m}$ . After the growth runs under the optimized condition, it was confirmed that the Si deposit is completely suppressed on the gas nozzles, as shown in Fig. 10 (b). The maintenance period of the nozzles under the optimized condition is increased more than 3 times or more

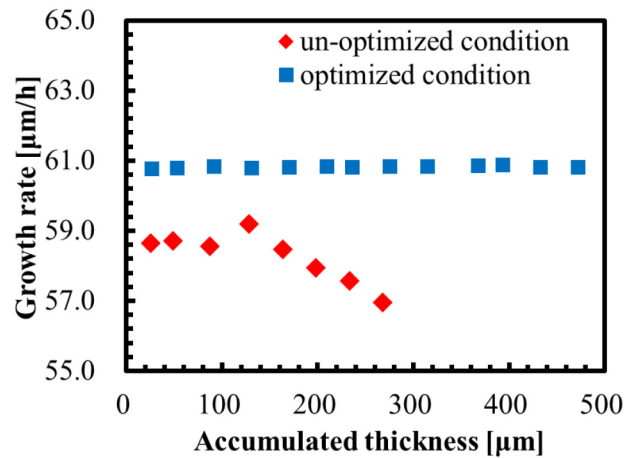


Fig. 11. Repeatability of growth rate of SiC films grown under optimized and un-optimized conditions. Same recipes were used in each growth runs, and additional treatments, such as reactor cleaning, were not performed within each growth runs. Under the optimized condition, gas flow and temperature at around gas inlet had been tuned.

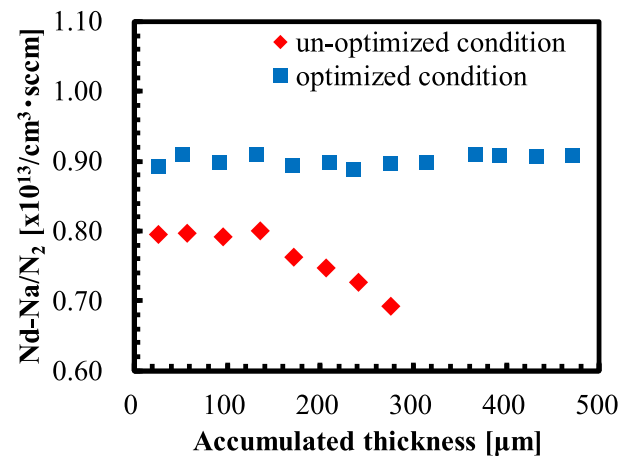


Fig. 12. Repeatability of doping concentration of the SiC films shown in Fig. 10. Since the target value of doping concentration was different between two growth runs, doping concentration value was divided by  $N_2$  flow rate. Under the optimized condition, gas flow and temperature at around gas inlet had been tuned.

compared with the epitaxial growth using the nozzles on which Si deposit was formed. Therefore, in order to improve the productivity and repeatability, the suppression of the Si deposit on the nozzles by optimizing condition is proposed.

Figure 13 shows schematic illustration of gas flow image at around the gas nozzle. In this figure, the gas flow images including the gas nozzle without Si deposit (a) and with Si deposit (b) are shown. Basically, the gas introduced from the nozzles into the reactor is divided to majority component that goes straight to the reaction space and minority component that goes around the nozzle. When epitaxial growth is performed under optimized condition, a gas component that goes around the nozzle seems to be straightened by surrounding gas, and goes to the reaction space. When epitaxial growth is performed under un-optimized condition, however, some of them seem to be reacted on the top of the gas nozzles and Si deposit is formed. Additionally, when the length of Si deposit is increased due to iteration of epitaxial growth, Si deposit

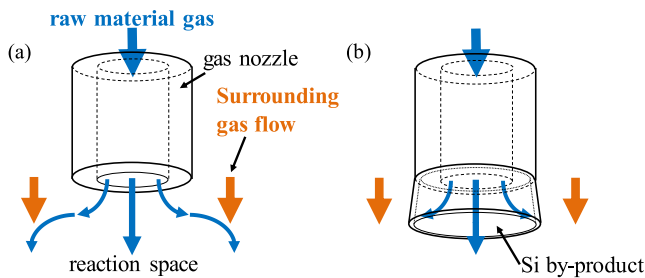


Fig. 13. Schematic illustration of gas flow image at around the gas nozzle. The gas flow images including the gas nozzle without Si deposit (a) and with Si deposit (b) are shown.

formed on the gas nozzles acts as a trap site of Si source gas as shown in Fig. 13 (b). In this situation, since the concentration of Si source gas introduced into the reactor is decreased with increasing accumulated thickness, decrease of thickness and doping concentration is thought to be observed.

#### IV. SUMMARY

Influence of by-product on epitaxial growth of 4H-SiC film was investigated and technique to reduce the harmful effect was proposed. High-speed rotation technology and optimized condition significantly suppressed the down-fall on the wafers and the fluctuation of growth rate and doping concentration. The results obtained in this study demonstrated that maintenance period and process stability can be dramatically improved.

#### REFERENCES

- [1] I.-H. Kang, S.-C. Kim, J.-H. Moon, W. Bahng, and N.-K. Kim, "Fabrication of a 600-V/20-A 4H-SiC schottky barrier diode," *J. Korean Phys. Soc.*, vol. 64, pp. 1886–1891, Jul. 2014.
- [2] K. Fukuda *et al.*, "Influence of processing and of material defects on the electrical characteristics of SiC-SBDs and SiC-MOSFETs," *Mater. Sci. Forum*, vols. 645–648, pp. 655–660, Apr. 2010.
- [3] N. Miura *et al.*, "4H-SiC power metal-oxide-semiconductor field effect transistors and schottky barrier diodes of 1.7 kV rating," *Jpn. J. Appl. Phys.*, vol. 48, no. 4S, 2009, Art. no. 04C085.
- [4] K. J. Han, B. J. Baliga, and W. J. Sung, "1.2 kV 4H-SiC split-gate power MOSFET: Analysis and experimental results," *Mater. Sci. Forum*, vol. 924, pp. 684–688, Jun. 2018.
- [5] S. Chowdhury, L. Gant, B. Powell, K. Rangaswamy, and K. Matocha, "Reliability and ruggedness of 1200V SiC planar gate MOSFETs fabricated in a high volume CMOS foundry," *Mater. Sci. Forum*, vol. 924, pp. 697–702, Jun. 2018.
- [6] A. Salemi, H. Elahipanah, C.-M. Zetterling, and M. Östling, "Conductivity modulated and implantation-free 4H-SiC ultra-high-voltage PiN diodes," *Mater. Sci. Forum*, vol. 924, pp. 568–572, Jun. 2018.
- [7] S. Asada, J. Suda, and T. Kimoto, "Effects of parasitic region in SiC bipolar junction transistors on forced current gain," *Mater. Sci. Forum*, vol. 924, pp. 629–632, Jun. 2018.
- [8] S.-H. Ryu, A. K. Agarwal, R. Singh, and J. W. Palmour, "1800 V NPN bipolar junction transistors in 4H-SiC," *IEEE Electron Device Lett.*, vol. 22, no. 3, pp. 124–126, Mar. 2001.
- [9] T. Kimoto, N. Miyamoto, and H. Matsunami, "Performance limiting surface defects in SiC epitaxial p-n junction diodes," *IEEE Trans. Electron Devices*, vol. 46, no. 3, pp. 471–477, Mar. 1999.
- [10] T. Katsuno, Y. Watanabe, H. Fujiwara, M. Konishi, T. Yamamoto, and T. Endo, "Effects of surface and crystalline defects on reverse characteristics of 4H-SiC junction barrier schottky diodes," *Jpn. J. Appl. Phys.*, vol. 50, no. 4S, 2011, Art. no. 04DP04.
- [11] K. Konishi *et al.*, "Effect of stacking faults in triangular defects on 4H-SiC junction barrier Schottky diodes," *Jpn. J. Appl. Phys.*, vol. 52, Mar. 2013, Art. no. 04CP05.
- [12] M. Skowronski and S. Ha, "Degradation of hexagonal silicon-carbide-based bipolar devices," *J. Appl. Phys.*, vol. 99, Jan. 2006, Art. no. 011101.
- [13] H. Das, S. Sunkari, J. Justice, H. Pham, and K. S. Park, "Effect of defects in silicon carbide epitaxial layers on yield and reliability," *Mater. Sci. Forum*, vol. 963, pp. 284–287, Jul. 2019.
- [14] T. S. Sudarshan, T. Rana, H. Song, and M. V. S. Chandrashekar, "Trade-off between parasitic deposition and SiC homoepitaxial growth rate using halogenated Si-precursors," *ECS J. Solid-State Sci. Technol.*, vol. 2, no. 8, pp. N3079–N3086, 2013.
- [15] Y. Daigo, T. Watanabe, A. Ishiguro, S. Ishii, M. Kushibe, and Y. Moriyama. (Dec. 2020). *Reduction of Harmful Effect Due to By-Product in CVD Reactor for 4H-SiC Epitaxy. Presented at ISSM 2020*. [Online]. Available: <https://www.semiconportal.com/issm/index.html>
- [16] Y. Daigo, A. Ishiguro, S. Ishii, and H. Ito, "Reduction of surface and PL defects on n-type 4H-SiC epitaxial films grown using a high speed wafer rotation vertical CVD tool," *Mater. Sci. Forum*, vol. 924, pp. 108–111, Jun. 2018.
- [17] H. Tsuchida I. Kamata, T. Miyazawa, M. Ito, X. Zhang, and M. Nagano, "Recent advances in 4H-SiC epitaxy for high-voltage power devices," *Mater. Sci. Semicond. Process.*, vol. 78, pp. 2–12, May 2018.